The Effects of Ambient Conditions on Solvent-Nanotube Dispersions: Exposure to Water and Temperature Variation

Zhenyu Sun[1,2], Ian O'Connor[1], Shane D Bergin[1] and Jonathan N Coleman[1,2]*

[1]*School of Physics, Trinity College Dublin, University of Dublin, Dublin 2, Ireland*

[2]*Centre for Research on Adaptive Nanostructures & Nanodevices CRANN, Trinity College Dublin, University of Dublin, Dublin 2, Ireland*

Abstract

Dispersions of single walled nanotubes in N-methyl-2-pyrrolidone have been exposed to water and variations in storage temperature. The subsequent degradation of dispersion quality has been monitored using sedimentation, UV-vis-NIR, and AFM measurements. Four parameters derived from AFM; the root-mean-square bundle diameter, the total number of dispersed objects (individuals and bundles) per unit volume of dispersion, the number fraction of individual nanotubes, and the number of individual nanotubes per unit volume of dispersion were used to quantitatively characterize the dispersion quality as a function of water content and storage temperature. In addition the positions of the nanotube absorption peaks were used to track dispersion quality, with redshifts taken as an indication of aggregation. It was found that water can rapidly shift the dispersion to a new but more aggregated equilibrium state. In particular the population of individual nanotubes falls to zero for relatively low amounts of added water. The dispersion quality decreases with increasing water content, reaching a plateau for all metrics by 20 vol% added water. In addition, it was also identified that low temperature treatment, i.e. -16, -18, -20, and -22 °C (all above the freezing point of NMP) does not influence the dispersion quality and stability regardless of the standing time. However, freezing (-80 °C) or heating (80 °C) the dispersion leads to a substantial degradation of the dispersion quality and stability.

1.0 Introduction

Stable, high quality dispersions of single-walled carbon nanotubes (SWNTs) are of interest for both fundamental research and practical applications. To achieve maximum dispersion quality, control of the interaction between nanotube and surrounding solvent is critical. This can be achieved by two major strategies: (1) covalent functionalization of the nanotube sidewall by oxidation, followed by reactions with

atoms or molecules such as fluorine,[1] alkanes,[2] diazonium salts,[3] or by ionic modification,[4] and (2) non-covalent stabilization by interaction with certain solvents,[5-13] surfactants,[14-20] polymers,[21-23] and biomolecules, such as DNA[24,25] and peptides.[26,27] Due to the undesirable disruption of nanotube intrinsic electronic structure and properties by covalent modification, the latter approach has become the most widely used to disperse SWNTs. Dispersion in solvents has an esthetic appeal due to its simplicity, nevertheless, the complete set of criteria for SWNT dispersions in solvents has not been fully understood. It has been reported that good amide solvents for dispersing nanotubes are usually characterized by strong hydrogen bond acceptance basicity, high values of solvochromic parameters, and weak hydrogen bond donation ability.[28,29] Alternatively, our recent results showed that nanotube dispersability is maximized in solvents whose surface energy matches that of graphitic surfaces (~70 mJ/m^2).[30] This criterion has also been shown to apply to graphene dispersions[31].

To date, *N*-Methyl-2-pyrrolidone (NMP) is one of the most promising solvents for dispersing both nanotubes[12,30] and graphene[31]. In fact previous studies have shown the enthalpy of mixing for nanotubes dispersed in NMP to be slightly negative suggesting nanotubes form thermodynamic solutions in NMP.[30] After mild centrifugation, a stable nanotube dispersion in NMP can be obtained with a concentration as high as ~0.05 mg/mL.[12,30] In our previous work,[12,19,20] we established several metrics to quantify dispersion quality and debundling efficiency, such as the root-mean-square bundle diameter (D_{rms}), the total number of dispersed objects (individuals and/or bundles) per unit volume of dispersion (N_{Tot}/V), the number fraction of individual nanotubes (N_{Ind}/N_{Tot}), and the number of individual nanotubes per unit volume of dispersion (N_{Ind}/V).

However, it is currently unknown how environmental conditions affect the quality of nanotube dispersions in solvents such as NMP. For example, NMP is known to be a relatively hygroscopic solvent. As such, under less than rigorous storage conditions, NMP may take up significant quantities of water. It is not known whether the presence of such dissolved water will affect the quality of nanotube dispersions. However, an adverse consequence may be expected by analogy with the effects of water on some inorganic nanowire dispersions.[32]

Alternatively, under certain circumstances, nanotube dispersions may need to be processed under conditions of either reduced or elevated temperature. This brings about another question; what will happen as the dispersion is subjected to non-ambient temperatures, perhaps during transportation of storage? Kim et al. showed that once surfactant-stabilised dispersions of isolated SWNTs are freeze-dried they cannot be re-dispersed in water, instead forming SWNT aggregates.[33] It is not known whether the same effects occur for nanotubes dispersed in organic solvents. In addition, most organic solvents have far lower freezing

points than water. Does this mean that solvent dispersed nanotubes can withstand low temperature conditions before, or even after, freezing treatment?

To clarify these questions, we designed a series of experiments to quantitatively investigate the effect of water content and temperature changes on the quality of nanotube dispersions in NMP. We select NMP as a representative organic solvent for this research because of its availability and exceptional dispersing ability for SWNTs as well as its good compatibility with many other solvents. The dispersion quality was tracked using the four metrics by AFM as well as other characterization methods including UV-vis-NIR spectroscopy and sedimentation studies.

2.0 Experimental

Purified single-walled nanotubes (HiPCO) were purchased from Carbon Nanotechnologies, Inc., and used without further treatment (lot no. PO342). *N*-methyl-2-pyrrolidone (NMP) (Product number: 242799) was purchased from Sigma-Aldrich and used as supplied. According to previously published procedures,[12] a dispersion of pristine SWNTs in NMP was prepared at an initial concentration of 0.1 mg/mL by sonicating for 2 min using a high-power ultrasonic tip processor (Vibra Cell CVX; 750 W, 20%, 20 kHz). The dispersion was subsequently kept in a sonic bath (Model Ney Ultrasonic) for 4 hr, followed by 1 min high-power sonication again. Shortly afterward, UV-vis-NIR characterisation was performed. Micro-scale aggregates were removed by a mild centrifugation (CF) step for 90 min at 5500 rpm (~3000 g) followed by decantation of the supernatant. The UV-vis-NIR absorbance was recorded for the dispersion after CF. Calculating the ratio of absorbance at a fixed wavelength (660 nm) before and after CF allows us to estimate the concentration of SWNTs retaining in the supernatant. The dispersion was then diluted with NMP to a nanotube concentration (C_{NT}) of 0.01 mg/mL and homogenized with 2 min sonic tip. This dispersion was subsequently used as a stock dispersion.

The effect of water on SWNT-NMP dispersions was investigated by adding varying quantities of deionised water (without sonication) to the stock dispersion described above. Dispersions with water volume fractions of 0.2%, 0.5%, 2%, 3%, 5%, 10% and 20% were produced. These dispersions were characterized by optical absorbance and AFM measurements. In addition, low temperature experiments were performed on samples of the stock dispersion which were kept in a freezer for either 30 min or 10 hr at temperatures ranging from -16 to -80 °C. High temperature experiments were performed on samples of the stock dispersion heated to 50 and 80 °C, for 30 min under argon environment. Optical absorbance, and AFM measurements for temperature-treated samples were carried out when they had returned to room temperature.

UV-vis-NIR measurements were made with a Varian Cary 6000i. Atomic Force Microscopy (AFM) samples were prepared by soaking functionalized silicon substrates in the dispersions for some 10 min. Then, they were rinsed with methanol and blown dry with high pressure compressed air. Tapping mode AFM (Multimode Nanoscope IIIA), using point probe silicon cantilevers (force constant = 42 Nm^{-1} & resonant frequency = 330 kHz) was performed on each sample. In each case, a distribution of SWNT diameters was recorded and statistical data extracted.

3.0 Results and discussion

For them to demonstrate maximum utility, solutions of carbon nanotubes in solvents such as NMP must be stable in a range of different environments. For example they must be stable against aggregation in response to environmental variations such as changes in temperature or humidity. To examine this we have investigated the aggregation state of NMP-nanotube solutions both after exposure to water and after heating and cooling.

3.1 Influence of Water

In order to investigate the influence of water on NMP-SWNT solutions, we introduce varying quantities of water in a controlled manner. We then monitor the temporal stability of the dispersions through sedimentation measurement. In addition, we probe the quality of the dispersion through absorption spectroscopy. Finally we quantify the state of the dispersion by AFM measurements on nanotube bundles deposited on Si/SiO_2 surfaces. Using statistical analysis this information can be transformed to give a number of dispersion quality metrics.

3.1.1 Sedimentation

The stability of the dispersions diluted with water can be crudely estimated simply by observation. Surprisingly, it was found that the dispersion remained visually homogeneous, with no discernible sedimentation over short time periods, even when water was added to a stock dispersion (initial C_{NT}=0.01 mg/mL) at a 50% volume ratio. To further investigate this, we performed quantitative, in-situ sedimentation measurements on dispersions with different added water contents. These experiments involve the measurement of the sample absorbance (650 nm) as a function of time in a specially built apparatus.[34] Figure 1 shows the sedimentation spectra for a series of water dilutions. For the dilutions by ≤10 vol% water, the absorbance remained extremely stable over 15 days implying that no sedimentation occurred. In the case of the dilution by 20 vol% water, the absorbance remained constant over the first week before falling slightly, suggesting the occurrence of aggregation or sedimentation. After 12 days, the absorbance started to decrease abruptly, indicating the onset of aggregation/sedimentation. Moreover, as

the water content was increased to 50 vol%, after 2 days, severe sedimentation can be clearly identified in the dilution. Further quantitative analysis will be discussed in the following AFM section.

3.1.2 UV-vis-NIR

Figure 2 shows representative absorption spectra of NMP for various water dilutions. Well-resolved optical absorption peaks in the ranges of 800-1600 nm and 550-900 nm (S_{11} and S_{22}) for semiconducting tubes, and 400-600 nm for metallic tubes (M_{11}) correspond to transitions between symmetric van Hove peaks in the nanotube density of states.[35] The decrease of optical absorbance as the increase of water or NMP arises from the reduction of nanotube concentration by dilution. In the case of the water dilutions, their absorption intensity appears similar to that of equivalent NMP dilutions.

Dilution with water results in an unambiguous red-shift which increases with increasing water dilution volume. We plot peak positions for selected S_{11}(~ 1310 nm), S_{22} (~ 741 nm), and M_{11} (~416 nm) peaks versus water dilution volume, as shown in Figure 2 B-D. The redshift is clearly apparent with a large shift in the S_{11} peak position around 5 vol% water. By the addition of 20 vol% water, redshifts of 4.8 nm (~ 3.95 meV), 1.4 nm (~3.15 meV), and 0.8 nm (~5.72 meV) had been observed in the S_{11}, S_{22}, and M_{11} regions respectively. We believe there are two interrelated explanations for the observed redshift. As the water content increases beyond 2.5 vol%, significant quantities of water begin to penetrate to the nanotube-NMP interface. This is known to result in a redshift in the nanotubes' optical transitions.[36,37] It is actually quite surprising that the water can displace NMP molecules to reach the interface given the strong affinity of NMP to nanotube surfaces.[30] Nevertheless, as we shall see below, once the water begins to reach the surface, the nanotubes begin to aggregate. It should be pointed out that the aggregation process in itself can induce a redshift[35]. Thus the redshift we observe is probably due to a combination of adsorbed water and the resultant aggregation.

3.1.3 AFM

Sedimentation and UV-vis-NIR measurements have provided qualitative information on the stability of the dilutions. However, the dispersion quality of the dilutions is still unclear. To unravel the behavior of the nanotubes in the dilutions, we carried out AFM characterization of our samples in order to gather quantitative information about the size distribution of nanotube bundles in the dilutions. Typical AFM images of nanotubes deposited from dilutions onto SiO_2 are shown in Figures S1A and B. The bundle diameter distributions were obtained for each sample from the heights of 100 randomly chosen

objects. Note that the diameter distribution of water dilutions broadens and shifts to higher values with the increase of water content (Figure 3).

Using the diameter distributions, we can calculate four related parameters that can be used to quantify the state of the dispersion as a function of dilution volume[20]. These are the root-mean-square bundle diameter (D_{rms}), the total number of bundles/individual nanotubes per unit volume (N_{Tot}/V), the number fraction of individual nanotubes (N_{Ind}/N_{Tot}) and the total number of individual nanotubes per unit volume (N_{Ind}/V). The measurement/calculation of these quantities has been described elsewhere.[12] These four parameters have been calculated and are plotted versus dilution (NMP or water) volume fraction in Figure 4. It can be observed that N_{Ind}/N_{Tot}, N_{Ind}/V, N_{Tot}/V all increase while D_{rms} decreases with the addition of NMP. This is reflective of the slight improvement in dispersion quality expected after small reductions in concentration.[12]

On addition of water however, we see a completely different effect. As the water content is added, N_{Ind}/N_{Tot}, N_{Ind}/V, N_{Tot}/V all *decrease* while D_{rms} *increases*. These changes are indicative of a degradation in dispersion quality on addition to water. This shows clearly that exposure to water causes nanotubes and bundles to aggregate. For all metrics except N_{Ind}/N_{Tot}, aggregation occurs on addition of as little as 0.2 vol% water. In this case the lack of change of N_{Ind}/N_{Tot} is coincidental, a reflection of the fact that N_{Ind}/V and N_{Tot}/V have changed by similar amounts. Above 2 vol%, the pace of aggregation increases, reaching a plateau for all metrics by 20 vol% water added. We note that on addition to 20 vol% water, D_{rms} had increased by 80% to nearly 4.5 nm while N_{Tot}/V had decreased by 70% to 0.4 μm^{-3}. Perhaps more importantly, both metrics representing the population of individual nanotubes had crashed to zero on the addition of 20 vol% water. In essence no individual NTs can be identified by close examination of the sample using AFM. This water-inducing re-aggregation has also been observed for the dispersion of $Mo_6S_{4.5}I_{4.5}$ nanowires.[32] This effect will obviously have catastrophic consequences for dispersions stored in an environment where significant water contamination can occur.

In the above section, we showed that the 5 vol% water dilution can remain stable against sedimentation over the course of 15 days. However, the behavior of its dispersion quality over that timeframe is still unknown. As such, we carried out another AFM measurement for the sample after 7 day incubation. The calculated values of the four metrics are embedded in Figure 4. It was found that after 7 days all four metrics remained close to their values as measured instantly after water addition. From this scenario, we can conclude that the effect of water on the nanotube dispersion is to very rapidly shift the equilibrium to a more aggregated state. The level of aggregation in this new equilibrium state is then dependent on the amount of water added.

We also made a preliminary investigation into some other common solvents regarding their effects on the dispersion of nanotubes in NMP. As 20% volume fraction of ethanol, acetone, cyclohexanone, tetrahydrofuran, or toluence was added, the nanotube dispersion remained stable against visual sedimentation for at least 20 days. While for the dilution with 20 vol% methanol, discernible sedimentation occurred after 10 days. Moreover, in the case of 20 vol% 2-chlorophenol dilution, nanotubes precipitated instantaneously from the bulk dispersion. We consider that the introduction of a third phase in the nanotube dispersions may result in a "competitive" process involving several interactions including SWNT-SWNT, NMP-SWNT, NMP-solvent, and solvent-SWNT interactions. Put simply, this changes both the solvent surface energy and the solvent-nanotube interfacial energy resulting in a significant increase in the enthalpy of mixing[30]. This change makes aggregation favorable over continued dispersion.

3.2 Temperature influence

3.2.1 UV-vis-NIR

In order to study temperature variation effects on the dispersion stability, the stock dispersion was kept at different temperatures varying from 80 to -80 °C for times varying from 30 min to 10 hr. We note that no visual change can be discerned for samples treated at temperatures from -16 to -22 °C. In addition, UV-vis-NIR absorption spectra for these samples (Figure 5A) illustrate that their spectra shape and intensity are almost identical. This may imply that the dispersion can remain stable without significant aggregation provided that the sample is not allowed to freeze. However, the absorption spectrum of the -80 °C treated sample exhibits relatively lower peak intensity. In addition, visible sedimentation occurred several hours later after this sample recovered to room temperature as shown in Figure S2C. This indicates that freezing treatment for the dispersant can induce severe aggregation and sedimentation of nanotubes consistent with the results for surfactant system demonstrated by Kim et al.[33] The reason for this phenomenon is at present unclear. We tentatively attribute this to the isotropic alignment of NMP molecules due to freezing treatment and the resulting reduction of the interaction between nanotube surfaces and NMP. As a result, isolated NTs with less NMP absorbant approach each other, predominantly driven by van der Walls forces resulting in aggregation. Alternatively, the formation of the initial ice crystallites will result in the reduction of the liquid volume and the associated increase in nanotube concentration. Such concentration increases are known to be accompanied by aggregation.[12,13] The redispersibility of the -80 °C-treated sample was further checked in this work. We found that it can be redispersed by high sonication power (1 min sonic tip), however, 1.5 hr mild sonication bath cannot

achieve homogeneous dispersion. This suggests that large NT aggregates predominate in the dispersion due to re-aggregation induced by freezing treatment.

For the samples stored between -22 °C and 20 °C no visible changes in dispersion quality were observed. In addition the absorption spectra were identical. In the case of the 50 °C sample, the optical spectral shape and intensity remains almost unchanged, implying no occurrence of servere aggregation. However, visible sedimentation took place when the dispersion was subjected to 80 °C for 30 min. This can clearly be reflected by the reduction of the intensity throughout the optical spectrum. Moreover, we also plotted peak positions for selected S_{11}(~ 1310 nm), S_{22} (~ 741 nm), and M_{11} (~416 nm) peaks versus temperature, as shown in Figure 5 B-D. No redshift occurred for dispersions treated at temperatures varying from -16 to -22 °C regardless of exposure time. Small redshifts were observed for the S_{22} and M_{11} peak positions for the dispersion subjected to 50 °C for 30 min. This small redshift suggests the onset of aggregation occurs somewhere slightly below 50°C. However, significant redshifts were observed for the samples stored at 80 and -80 °C suggesting significant levels of aggregation for samples stored at these more extreme temperatures.

3.2.2 AFM

To gain more insight into temperature variation effects on the dispersion quality, we performed AFM measurements for those temperature treated samples. As can been seen from Figure 6, the diameter distributions extracted from AFM analyses on 100 random objects are similar for samples treated in the range of 20 to -22 °C, however, for the sample treated at 50, 80, and -80 °C, the diameter distribution broadens and shifts to higher values. A typical AFM image of nanotubes deposited from the sample subjected to -80 °C onto Si/SiO_2 can be clearly observed in Figure S1C. Using the diameter distributions, the four metrics (D_{rms}, N_{Ind}/N_{Tot}, N_{Ind}/V, N_{Tot}/V) were calculated and presented in Figure 7 as a function of temperature. Note that these four metrics remain constant within error for samples even subjected to low T from -16 to -22 °C for 30 min. To check the low-temperature treatment time influence on the dispersion, the stock dispersion was kept under -22 °C for 10 hr. Surprisingly, no change occurred with respect to the four metrics. This shows that low-T treatment in the liquid phase does not induce aggregation. However, as the sample was freezing-treated at -80 °C for 10 hr, the value of D_{rms} significantly increased to 3.72±0.32 as compared to 2.63±0.15 nm before the treatment, while the values of N_{Ind}/N_{Tot}, N_{Ind}/V, N_{Tot}/V fell by a factor of two. Therefore, we can conclude that the dispersion can sustain low-T conditions (>-24 °C) with no change of the dispersion quality, however, freezing treatment (<-24 °C) results in an extreme deterioration of the dispersion quality and stability.

For dispersions treated at higher temperatures of 50 and 80 °C for 30 min, the value of D_{rms} had increased by 41 and 66% to 3.71±0.21 and 4.37±0.18 nm, while N_{Tot}/V had decreased by 50 and 64% to 0.7 and 0.5 μm^{-3} respectively. This clearly indicates that high T can result in a significant degradation of the dispersion quality. This seems surprising because we expect[30] the NMP-NT dispersion at 0.01 mg/mL to behave as a solution. Normally, solubility tends to increase with increasing temperature as the entropic component of the free energy of mixing plays a larger role. However, this is unlikely to apply here as the entropy of mixing is extremely low for these extremely large molecules. We may in fact be witnessing a temperature dependence of the enthalpy of mixing. In solutions, the enthalpy of mixing is controlled by the balance of the solubility parameters[38] of solvent and solute. It is known that the solubility parameters of solvents are temperature dependent[39,40]. In fact, by calculating the temperature variation[39] of the dispersion, polar and Hydrogen bonding components of the solubility parameter (Hansen parameters) of NMP, one can estimate that the solubility parameter of NMP changes from ~23 $MPa^{1/2}$ to 21.7 $MPa^{1/2}$ as the temperature increases from 20 ^oC to 80 ^oC. As the measured enthalpy of mixing of SWNTs in NMP is only very slightly negative (Flory-Huggins parameter = -0.074)[30], this temperature induced change in the solubility parameters may be enough to shift the enthalpy of mixing from being slightly negative to slightly positive, causing aggregation. However, to fully understand this, more work is required into the nature of the dispersed state of nanotubes in solvents such as NMP.

4.0 Conclusions

In summary, we have made a quantitative experimental analyses of water and temperature effects on SWNT dispersions in NMP (C_{NT}=0.01 mg/mL). It was found that a third-phase solvent (i.e. water) can rapidly shift the dispersion to a new but more aggregated equilibrium state dependent on the amount of water added. Aggregation occurs on addition of as little as 0.2 vol% water. Above 2 vol%, the pace of aggregation increases, reaching a plateau for all dispersion quality metrics by 20 vol% water added. On addition to 20 vol% water, D_{rms} had increased by 80% to nearly 4.5 nm while N_{Tot}/V had decreased by 70% to 0.4 μm^{-3}. Furthermore, the population of individual nanotubes had crashed to zero. UV-vis-NIR measurements show that dilution with water resulted in an unambiguous red-shift which increases with increasing water dilution volume. Temperature treatment studies demonstrate that the dispersion quality remained unchanged regardless of standing time as long as the NMP was not allowed to freeze. However, freezing of NMP (-80 °C) induced severe degradation of the dispersion coupling with a factor of two decrease of N_{Ind}/N_{Tot}, N_{Ind}/V, and N_{Tot}/V and a substantial increase of D_{rms}. Large aggregation/bundles then dominated the dispersion and only by using a high-power sonication tip can it be re-dispersed. In the

case of higher temperature experiments, the quality of dispersion degraded significantly with the increase of temperature beyond 50 ^{o}C. For example, as the dispersion was heated to 50 and 80 °C for 30 min, the value of D_{rms} increased by 41 and 66% to 3.71±0.21 and 4.37±0.18 nm, while N_{Tot}/V decreased by 50 and 64% to 0.7 and 0.5 μm^{-3} respectively. We believe that this work positively contributes to the understanding of nanotube dispersions and hope it will be useful in aiding the practical handling of nanotube dispersions.

Acknowledgment. The authors wish to thank Miss Jinghuan Li for her help in low temperature experiments, also thank SFI (through the Research Frontier Program) and the Centre for Research on Adaptive Nanostructures & Nanodevices for their financial support.

Supporting information: This consists of Figure S1-2, corresponding to typical AFM images for SWNT-NMP dispersions (C_{NT}=0.01 mg/mL) before and after 10 vol% dilution by H_2O and low temperature (-80 °C, 10 hr) treatment, photographs of the dispersion before and after low temperature (-80 °C, 10 hr) treatment.

References

(1) Mickelson, E. T.; Chiang, I. W.; Zimmerman, J. L.; Boul, P. J.; Lozano, J.; Liu, J.; Smalley, R. E.; Hauge, R. H.; Margrave, J. L. *J. Phys. Chem. B* **1999**, *103*, 4318.

(2) Boul, P. J.; Liu, J.; Mickelson, E. T.; Huffman, C. B.; Ericson, L. M.; Chiang, I. W.; Smith, K. A.; Colbert, D. T.; Hauge, R. H.; Margrave, J. L.; Smalley, R. E. *Chem. Phys. Lett.* **1999**, *310*, 367.

(3) Bahr, J. L.; Yang, J.; Kosynkin, D. V.; Bronikowski, M. J.; Smalley, R. E.; Tour, J. M. *J. Am. Chem. Soc.* **2001**, *123*, 6536.

(4) Chen, J.; Rao, A. M.; Lyuksyutov, S.; Itkis, M. E.; Hamon, M. A.; Cohn, R. W.; Eklund, P. C.; Colbert, D. T.; Smalley, R. E.; Haddon, R. C. *J. Phys. Chem. B* **2001**, *105*, 2525.

(5) Bahr, J. L.; Mickelson, E. T.; Bronikowski, M. J.; Smalley, R. E.; Tour, J. M. *Chem. Commun.* **2001**, 193.

(6) Furtado, C. A.; Kim, U. J.; Gutierrez, H. R.; Pan, L.; Dickey, E. C.; Eklund, P. C. *J. Am. Chem. Soc.* **2004**, *126*, 6095.

(7) Krupke, R.; Hennrich, F.; Hampe, O.; Kappes, M. M. *J. Phys. Chem. B* **2003**, *107*, 5667.

(8) Landi, B. J.; Ruf, H. J.; Worman, J. J.; Raffaelle, R. P. *J. Phys. Chem. B* **2004**, *108*, 17089.

(9) Liu, J.; Casavant, M. J.; Cox, M.; Walters, D. A.; Boul, P.; Lu, W.; Rimberg, A. J.; Smith, K. A.; Colbert, D. T.; Smalley, R. E. *Chem. Phys. Lett.* **1999**, *303*, 125.

(10) Umek, P.; Vrbanic, D.; Remskar, M.; Mertelj, T.; Venturini, P.; Pejovnik, S.; Mihailovic, D. *Carbon* **2002**, *40*, 2581.

(11) Maeda, Y.; Kimura, S.; Hirashima, Y.; Kanda, M.; Lian, Y. F.; Wakahara, T.; Akasaka, T.; Hasegawa, T.; Tokumoto, H.; Shimizu, T.; Kataura, H.; Miyauchi, Y.; Maruyama, S.; Kobayashi, K.; Nagase, S. *J. Am. Chem. Soc.* **2006**, *128*, 12239.

(12) Giordani, S.; Bergin, S. D.; Nicolosi, V.; Lebedkin, S.; Kappes, M. M.; Blau, W. J.; Coleman, J. N. *J. Phys. Chem. B* **2006**, *110*, 15708.

(13) Bergin, S. D.; Nicolosi, V.; Giordani, S.; de Gromard, A.; Carpenter, L.; Blau, W. J.; Coleman, J. N. *Nanotechnology* **2007**, *18*, 455705.

(14) Richard, C.; Balavoine, F.; Schulta, P.; Ebbesen, T. W.; Mioskowski, C. *Science* **2003**, *300*, 775.

(15) Moore, V. C.; Strano, M. S.; Haroz, E. H.; Hauge, R. H.; Smalley, R. E.; Schmidt, J.; Talmon, Y. *Nano Lett.* **2003**, *3*, 1379.

(16) Islam, M. F.; Rojas, E.; Bergey, D. M.; Johnson, A. T.; Yodh, A. G. *Nano Lett.* **2003**, *3*, 269.

(17) Wenseleers, W.; Vlasov, I. I.; Goovaerts, E.; Obraztsova, E. D.; Lobach, A. S.; Bouwen, A. *Adv. Func. Mater.* **2004**, *14*, 1105.

(18) Ishibashi, A.; Nakashima, N. *Chem. Eur. J.* **2006**, *12*, 7595.

(19) Bergin, S. D.; Nicolosi, V.; Cathcart, H.; Lotya, M.; Rickard, D.; Sun, Z.; Blau, W. J.; Coleman, J. N. *J. Phys. Chem. C* **2008**, *112*, 972.

(20) Sun, Z.; Nicolosi, V.; Rickard, D.; Bergin, S. D.; Aherne, D.; Coleman, J. N. *J. Phys. Chem. C* **2008**, *112*, 10692.

(21) Liu, J.; Rinzler, A. G.; Dai, H.; Hafner, J. H.; Bradley, R. K.; Boul, P. J.; Lu, A.; Iverson, T.; Shelimov, K.; Huffman, C. B.; Rodriguez-Macias, F.; Shon, Y. S.; Lee, T. R.; Colbert, D. T.; Smalley, R. E. *Science* **1998**, *280*, 1253.

(22) Chen, J.; Liu, H.; Weimer, W. A.; Halls, M. D.; Waldeck, D. H.; Walker, G. C. *J. Am. Chem. Soc.* **2002**, *124*, 9034.

(23) Kim, O. K.; Je, J.; Baldwin, J. W.; Kooi, S.; Pehrsson, P. E.; Buckley, L. J. *J. Am. Chem. Soc.* **2003**, *125*, 4426.

(24) Zheng, M.; Jagota, A.; Semke, E. D.; Diner, B. A.; Mclean, R. S.; Lustig, S. R.; Richardson, R. E.; Tassi, N. G. *Nat. Mater.* **2003**, *2*, 338.

(25) Cathcart, H.; S., Q.; Nicolosi, V.; Kelly, J. M.; Blau, W. J.; Coleman, J. N. *J. Phys. Chem. C* **2007**, *111*, 66.

(26) Witus, L. S.; Rocha, J. D.; Yuwono, V. M.; Paramonov, S. E.; Wersman, R. B.; Hartgerink, J. D. *J. Mater. Chem.* **2007**, *17*, 1909.

(27) Nicolosi, V.; Cathcart, H.; Dalton, A. R.; Aherne, D.; Dieckmann, G. R.; Coleman, J. N. *Biomacromolecules* **2008**, *9*, 598.

(28) Ausman, K. D.; Piner, R.; Lourie, O.; Ruoff, R. S.; Korobov, M. *J. Phys. Chem. B* **2000**, *104*, 8911.

(29) Marcus, Y. *Chem. Soc. Rev.* **1993**, *22*, 409.

(30) Bergin, S. D.; Nicolosi, V.; Streich, P. V.; Giordani, S.; Sun, Z. Y.; Windle, A. H.; Ryan, P.; Niraj, N. P. P.; Wang, Z. T.; Carpenter, L.; Blau, W. J.; Boland, J. J.; Hamilton, J. P.; Coleman, J. N. *Adv. Mater.* **2008**, *20*, 1.

(31) Hernandez, Y.; Nicolosi, V.; Lotya, M.; Blighe, F. M.; Sun, Z.; De, S.; McGovern, I. T.; Holland, B.; Byrne, M.; Gun'ko, Y. K.; Boland, J. J.; Niraj, P.; Duesberg, G. S.; Krishnamurthy, S.; Goodhue, R.; Hutchison, J.; Scardaci, V.; Ferrari, A. C.; Coleman, J. N. *Nature Nanotechnology (in press)* **2008**.

(32) Nicolosi, V.; McCarthy, D. N.; Vengust, D.; Mihailovic, D.; Blau, W. J.; Coleman, J. N. *European Physical Journal-Applied Physics* **2007**, *37*, 149.

(33) Kim, T. H.; Doe, C.; Kline, S. R.; Choi, S. M. *Adv. Mater.* **2007**, *19*, 923.

(34) Nicolosi, V.; Vrbanic, D.; Mrzel, A.; McCauley, J.; O' Flaherty, S.; McGuinness, C.; Compagnini, G.; Mihailovic, D.; Blau, W. J.; Coleman, J. N. *J. Phys. Chem. B* **2005**, *109*, 7124.

(35) O' Connell, M. J.; Bachilo, S. M.; Huffman, C. B.; Moore, V. C.; Strano, M. S.; Haroz, E. H.; Rialon, K. L.; Boul, P. J.; Noon, W. H.; Kittrell, C.; Ma, J.; Hauge, R. H.; Weisman, R. B.; Smalley, R. E. *Science* **2002**, *297*, 593.

(36) Hasan, T.; Scardaci, V.; Tan, P. H.; Rozhin, A. G.; Milne, W. I.; Ferrari, A. C. *J. Phys. Chem. C* **2007**, *111*, 12594.

(37) Strano, M. S.; Moore, V. C.; Miller, M. K.; Allen, M. J.; Haroz, E. H.; Kittrell, C.; Hauge, R. H.; Smalley, R. E. *J. Nanosci. Nanotech.* **2003**, *3*, 81.

(38) Hildebrand, J. H.; Prausnitz, J. M.; Scott, R. L. *Regular and related solutions*, First ed.; Van Nostrand Reinhold Company: New York, 1970.

(39) Hansen, C. M. *Hansen Solubility Parameters, A users handbook*; CRC Press: Boca Raton, 1998.

(40) Chee, K. K. *Journal of Applied Polymer Science* **1995**, *58*, 2057.

Figures

Figure 1. Sedimentation curves for SWNT-NMP dispersion at C_{NT}=0.01 mg/mL diluted by varying amount of H_2O.

Figure 2. A) Absorption spectra of SWNT-NMP dispersion at C_{NT}=0.01 mg/mL at a range of dilution volume fraction by H_2O and NMP. B) C) and D) Positions of selected peaks in the absorbance spectra as a function of H_2O volume fraction.

Figure 3. Histograms of bundle diameter for SWNT-NMP dispersion at C_{NT}=0.01 mg/mL at a range of dilution volume fraction by H_2O and NMP.

Figure 4. A) Root-mean-square bundle diameters (D_{rms}), B) number fraction of individual nanotubes (N_{Ind}/N_{Tot}), C) number of individual nanotubes per unit volume (N_{Ind}/V), and D) total number density of bundles/individuals (N_{Tot}/V) for SWNTs dispersed in NMP as a function of NMP or H_2O dilution volume fraction.

Figure 5. Absorption spectra of SWNT-NMP dispersion at C_{NT}=0.01 mg/mL at a range of temperature treatment.

Figure 6. Histograms of bundle diameter for SWNT-NMP dispersion at C_{NT}=0.01 mg/mL at a range of temperature treatment.

Figure 7. The four metrics of A) D_{rms}, B) N_{Ind}/N_{Tot}, C) N_{Ind}/V, and D) N_{Tot}/V for SWNTs dispersed in NMP (C_{NT}=0.01 mg/mL) as a function of temperature condition.

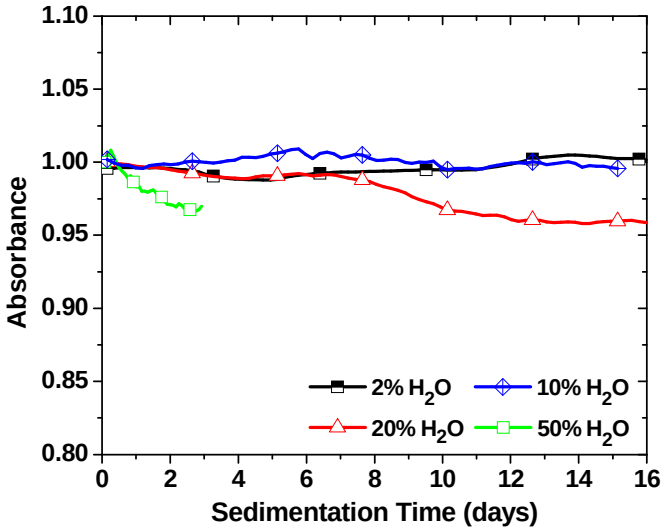

Figure 1. Sedimentation spectra of SWNT-NMP dispersion at C_{NT}=0.01 mg/mL diluted by varying amount of H_2O.

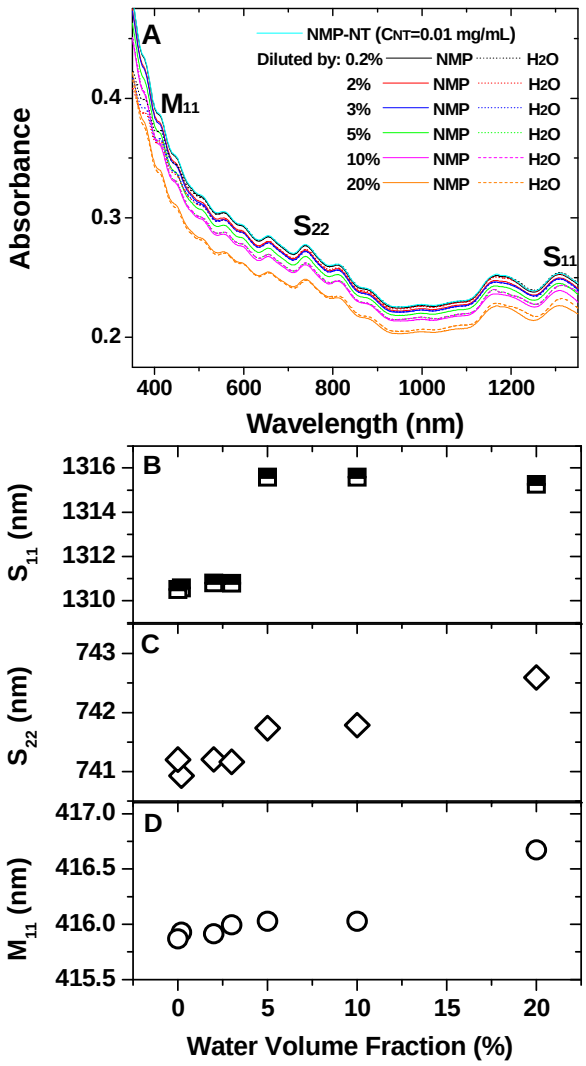

Figure 2. A) Absorption spectra of SWNT-NMP dispersion at C_{NT}=0.01 mg/mL at a range of dilution volume fraction by H_2O and NMP. B) C) and D) Positions of selected peaks in the absorbance spectra as a function of H_2O volume fraction.

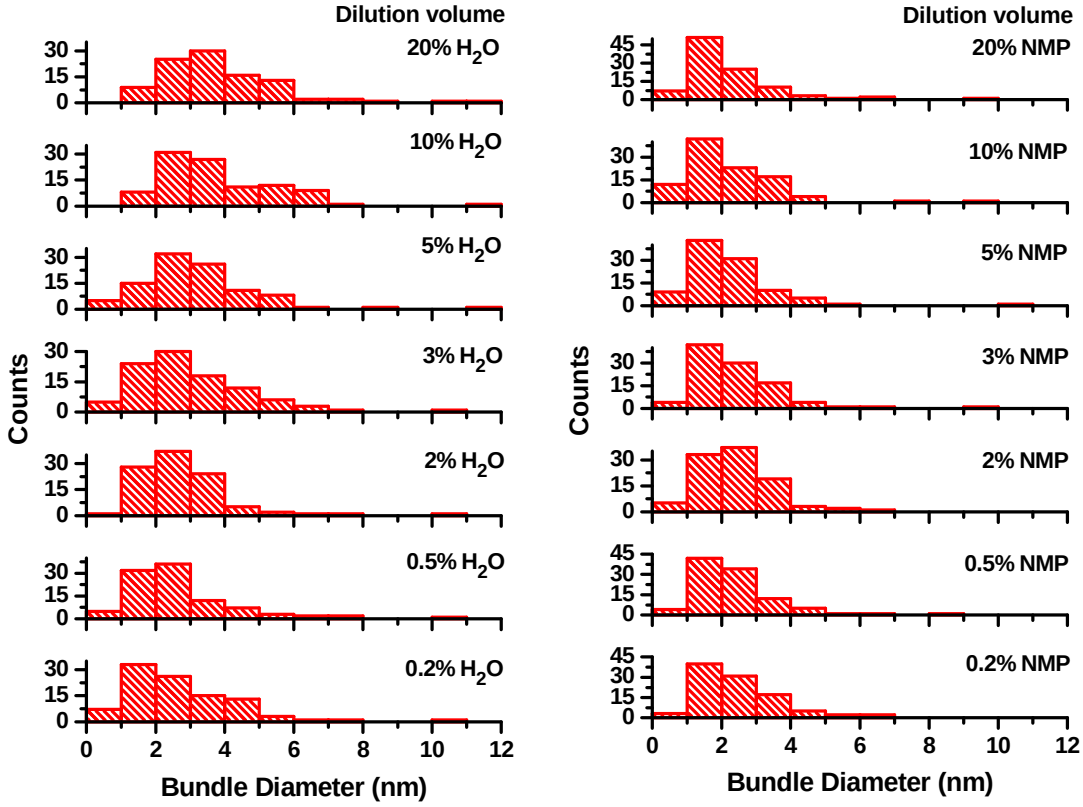

Figure 3. Histograms of bundle diameter for SWNT-NMP dispersion at C_{NT}=0.01 mg/mL at a range of dilution volume fraction by H_2O and NMP.

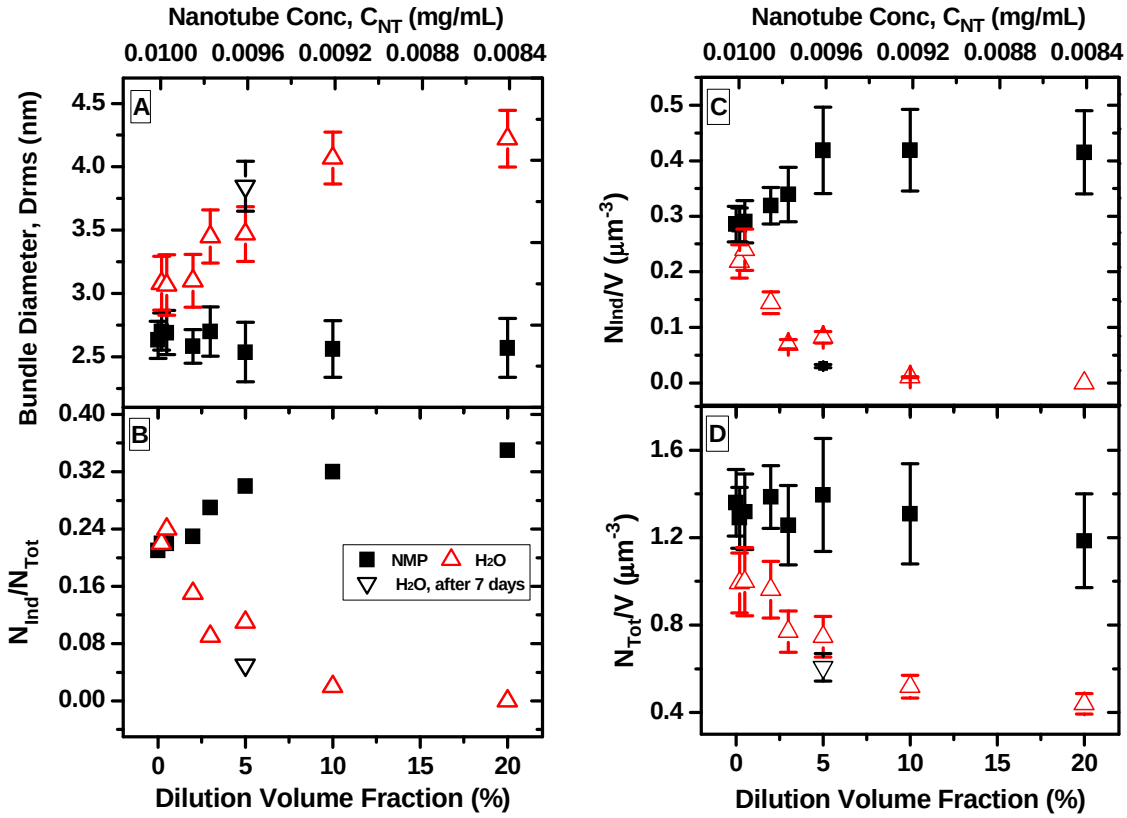

Figure 4. A) Root-mean-square bundle diameters (D_{rms}), B) number fraction of individual nanotubes (N_{Ind}/N_{Tot}), C) number of individual nanotubes per unit volume (N_{Ind}/V), and D) total number density of bundles/individuals (N_{Tot}/V) for SWNTs dispersed in NMP as a function of NMP or H_2O dilution volume fraction.

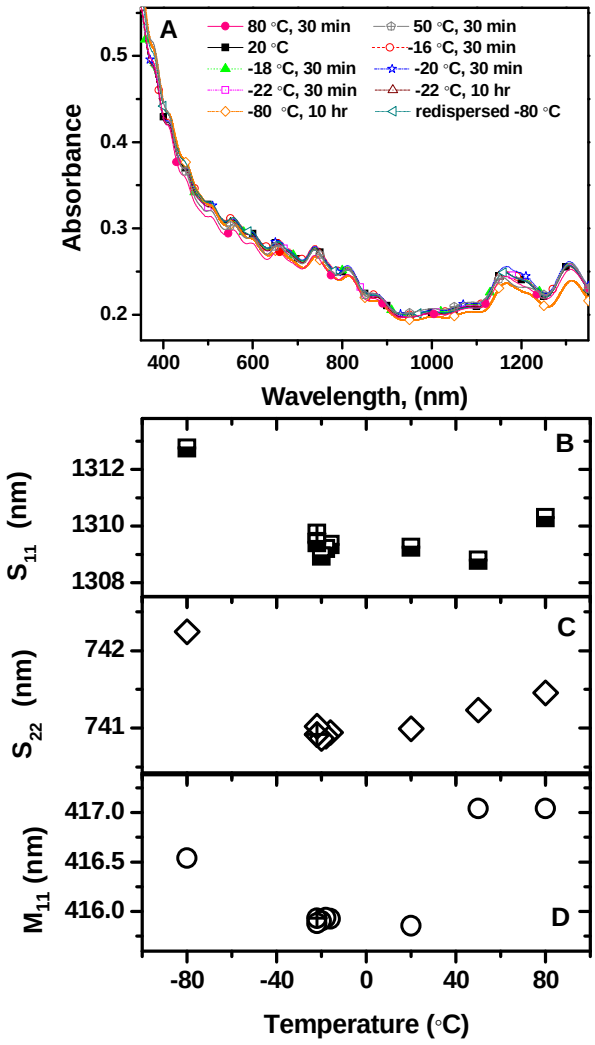

Figure 5. A) Absorption spectra of SWNT-NMP dispersion at C_{NT}=0.01 mg/mL at a range of temperature treatment. B) C) and D) Positions of selected peaks in the absorbance spectra as a function of temperature treatment, the crisis-circled symbol stands for 10 hr treatment at -22 °C.

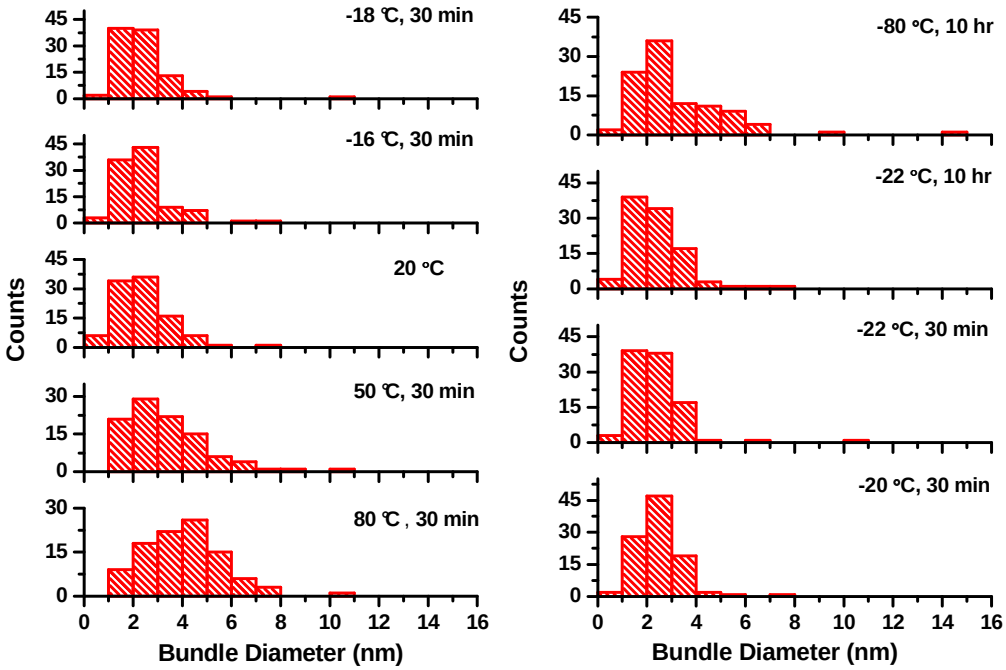

Figure 6. Histograms of bundle diameter for SWNT-NMP dispersion at C_{NT}=0.01 mg/mL at a range of low temperature treatment.

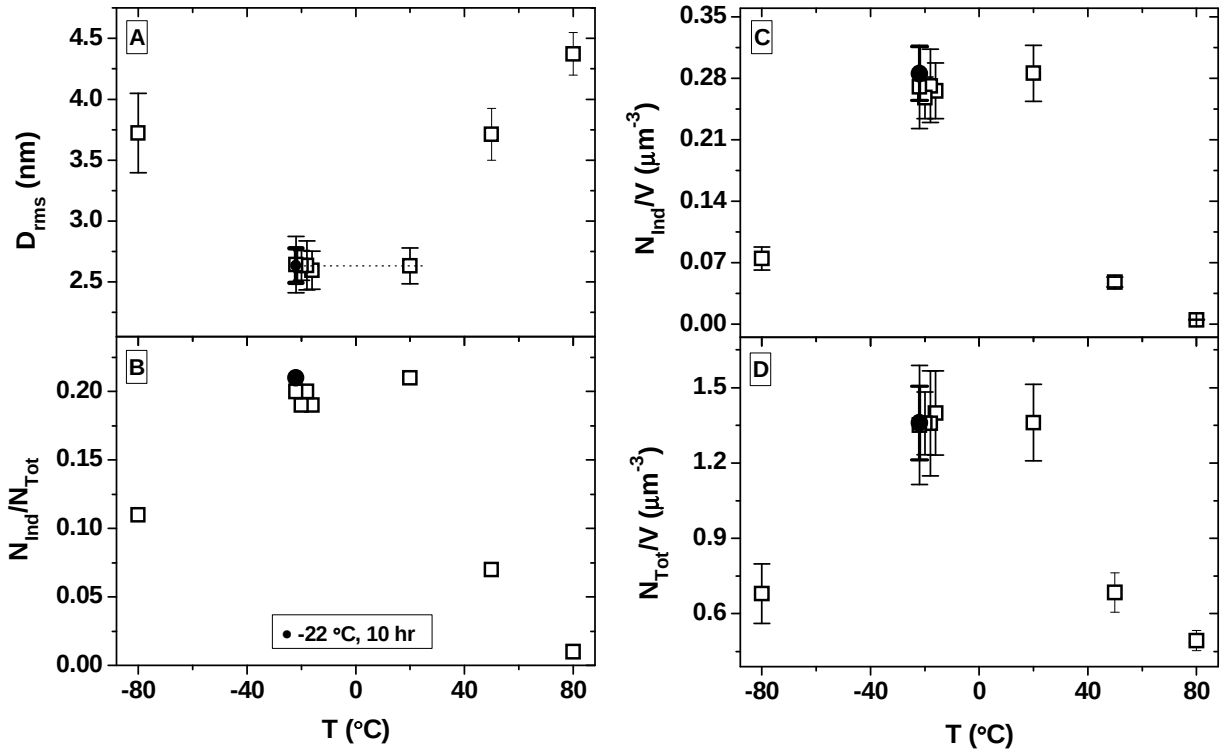

Figure 7. The four metrics of A) D_{rms}, B) N_{Ind}/N_{Tot}, C) N_{Ind}/V, and D) N_{Tot}/V for SWNTs dispersed in NMP (C_{NT}=0.01 mg/mL) as a function of temperature condition.